Electronic supplementary Information

For

Fluorination on non-photolabile dppz ligand improving Ru(II) complex-based photoactivated chemotherapy

Rena Boerhan,[ab] Weize Sun,[ab] Na Tian,[ab] Youchao Wang,[ab] Jian Lu,[ab] Chao Li, [a] Xuexin Cheng, [a] Xuesong Wang*[ab] and Qianxiong Zhou*[a]

[a]*Key Laboratory of Photochemical Conversion and Optoelectronic Materials, Technical Institute of Physics and Chemistry, Chinese Academy of Sciences, Beijing 100190, P. R. China. E-mail: xswang@mail.ipc.ac.cn (Xuesong Wang), zhouqianxiong@mail.ipc.ac.cn (Qianxiong Zhou).*

[b]*University of Chinese Academy of Sciences, Beijing 100049, P. R. China*

Figure S1. ^{1}H-NMR of [Ru(dppz)(py)$_4$](Cl)$_2$ (**1**) in deuterated water.....2
Figure S2. ^{1}H-NMR of complex **1** before and after irradiation 2
Figure S3. ^{1}H-NMR of [Ru(F-dppz)(py)$_4$](Cl)$_2$ (**2**) in deuterated water.....3
Figure S4. ^{1}H-NMR of complex **2** before and after irradiation 3
Figure S5. ^{1}H-NMR of [Ru(F$_2$-dppz)(py)$_4$](Cl)$_2$ (**3**) in deuterated water. 4
Figure S6. ^{1}H-NMR of [Ru(CF$_3$-dppz)(py)$_4$](Cl)$_2$ (**4**) in deuterated water. 4
Figure S7. ^{1}H-NMR of complex **4** before and after irradiation 5
Figure S8. Absorption spectra changes of complexes **1, 2, 4** in H$_2$O upon irradiation 5
Figure S9. ESI mass spectra of [Ru(dppz)(py)$_4$](Cl)$_2$ (**1**). 6
Figure S10. ESI mass spectra of **1** before and after irradiation 6
Figure S11. ESI mass spectra of [Ru(F-dppz)(py)$_4$](Cl)$_2$ (**2**). 7
Figure S12. ESI mass spectra of **2** before and after irradiation 7
Figure S13. ESI mass spectra of [Ru(F$_2$-dppz)(py)$_4$](Cl)$_2$ (**3**).....8
Figure S14. ESI mass spectra of **3** before and after irradiation 8
Figure S15. ESI mass spectra of [Ru(CF$_3$-dppz)(py)$_4$](Cl)$_2$ (**4**). 9
Figure S16. ESI mass spectra of**4** before and after irradiation 9
Figure S17. Percentage of apoptotic SKOV-3 cells treated with **1** (flow cytometry) 10
Figure S18. Percentage of apoptotic SKOV-3 cells treated with **2** (flow cytometry) 10
Figure S19. Percentage of apoptotic SKOV-3 cells treated with **4** (flow cytometry) 11
Figure S20. non-treated HeLa and SKOV-3 cells analysed by flow cytometry 11
Figure S21. Percentage of apoptotic HeLa cells treated with **1-4** (flow cytometry).....12
Figure S22. Annexin-FITC/PI staining of SKOV-3 cells treated with **1, 2, 4** (light).....13
Figure S23. Annexin-FITC/PI staining of SKOV-3 cells treated with 1, 2, 4 (dark).....14
Figure S24. Agarose gel electrophoresis pattern of pBR322 DNA treated with **1**, **2** and **4** 15

Table S1. IC$_{50}$ values of complexes **1-4** when culture medium was changed before irradiation. 15

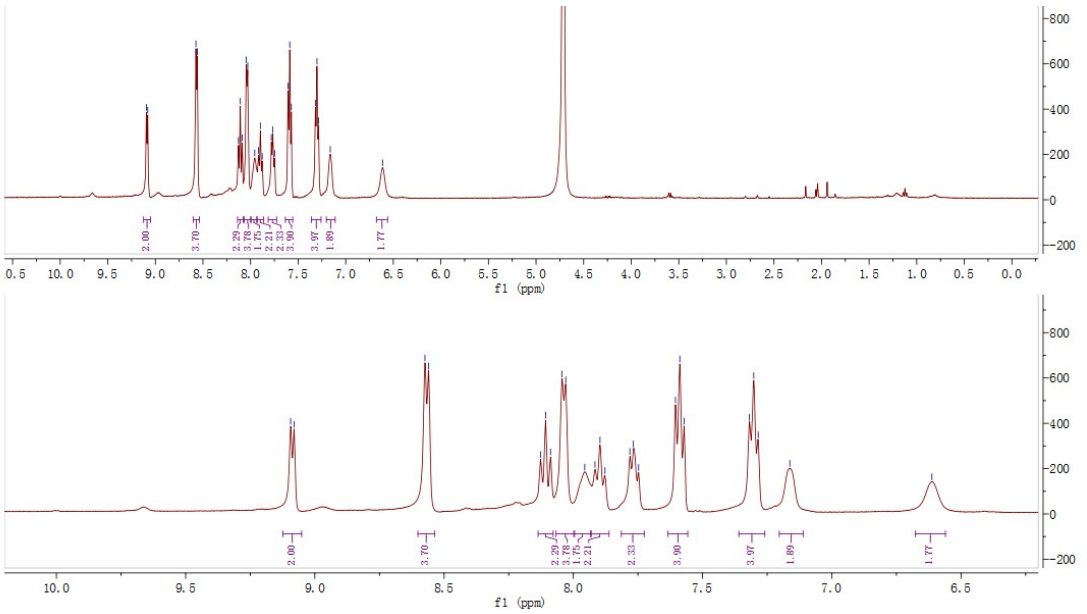

Figure S1. ^{1}H-NMR of $[Ru(dppz)(py)_4](Cl)_2$ (**1**) in deuterated water.

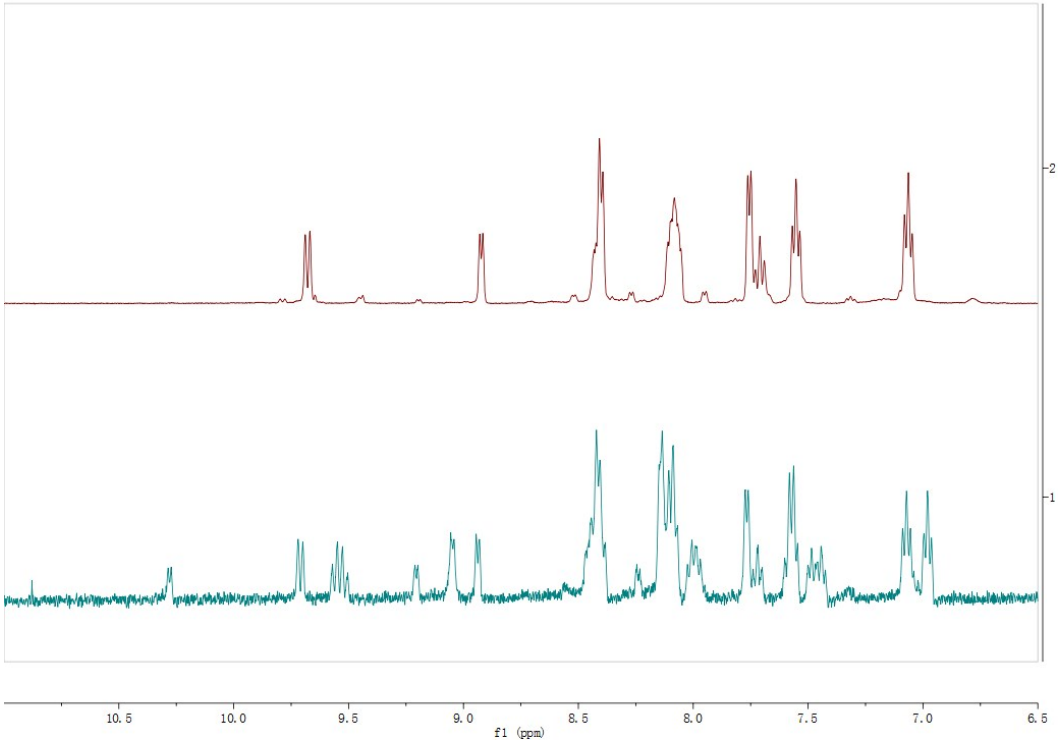

Figure S2. ^{1}H-NMR of complex **1** (top, in CD_3CN), and **1** after irradiation (bottom, 470 nm, 27 J/cm^2) in physiological saline. The irradiated sample was removed of solvent (and free pyridine in the process) and excess NaCl, and redissolved in CD_3CN.

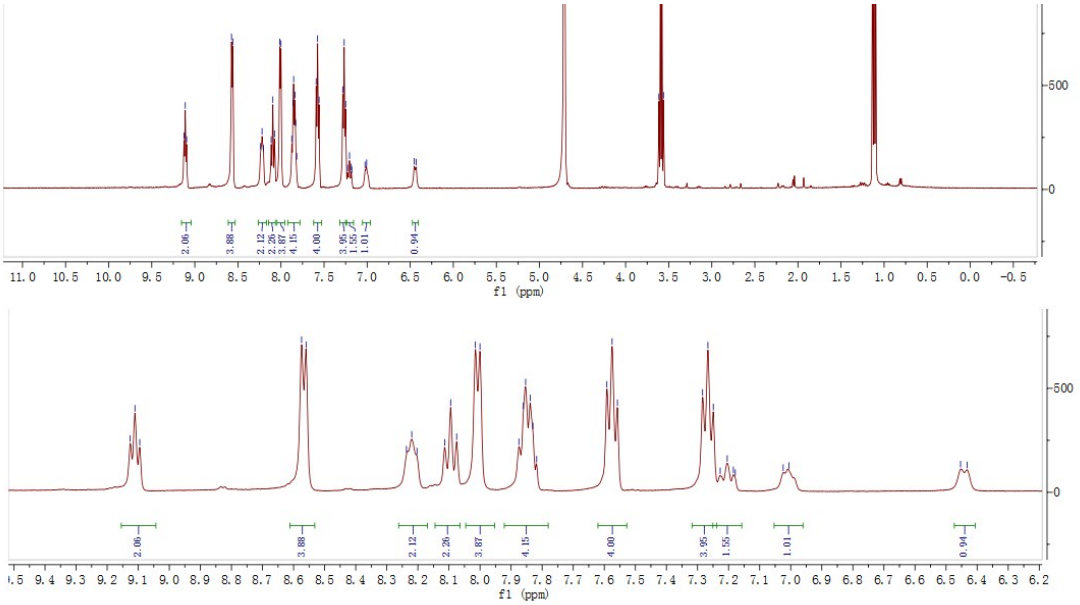

Figure S3. ^{1}H-NMR of [Ru(F-dppz)(py)$_4$](Cl)$_2$ (**2**) in deuterated water.

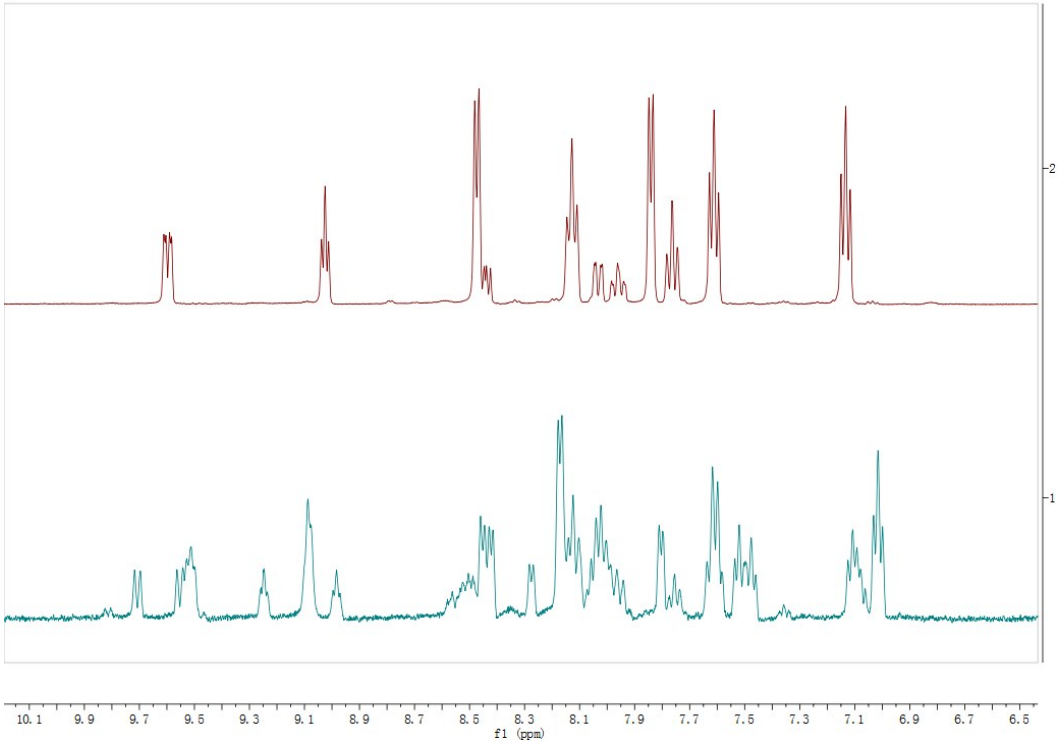

Figure S4. ^{1}H-NMR of complex **2** (top, in CD_3CN), and **2** after irradiation (bottom, 470 nm, 27 J/cm^2) in physiological saline. The irradiated sample was removed of solvent (and free pyridine in the process) and excess NaCl, and redissolved in CD_3CN.

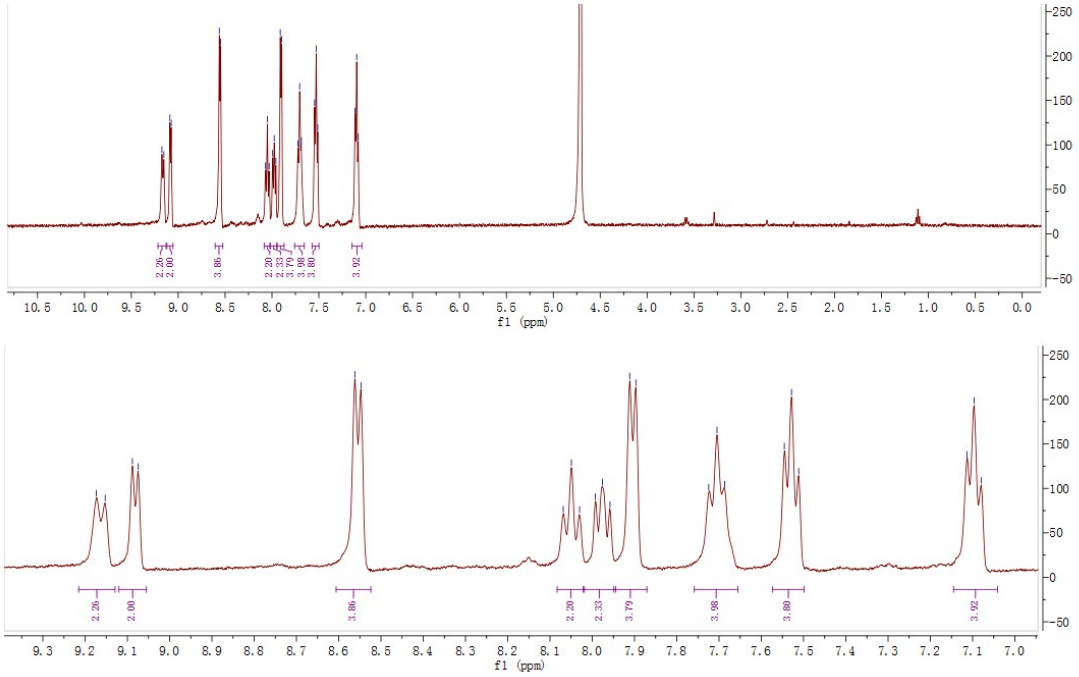

Figure S5. ^{1}H-NMR of [Ru(F_2-dppz)($py)_4$]($Cl)_2$ (**3**) in deuterated water.

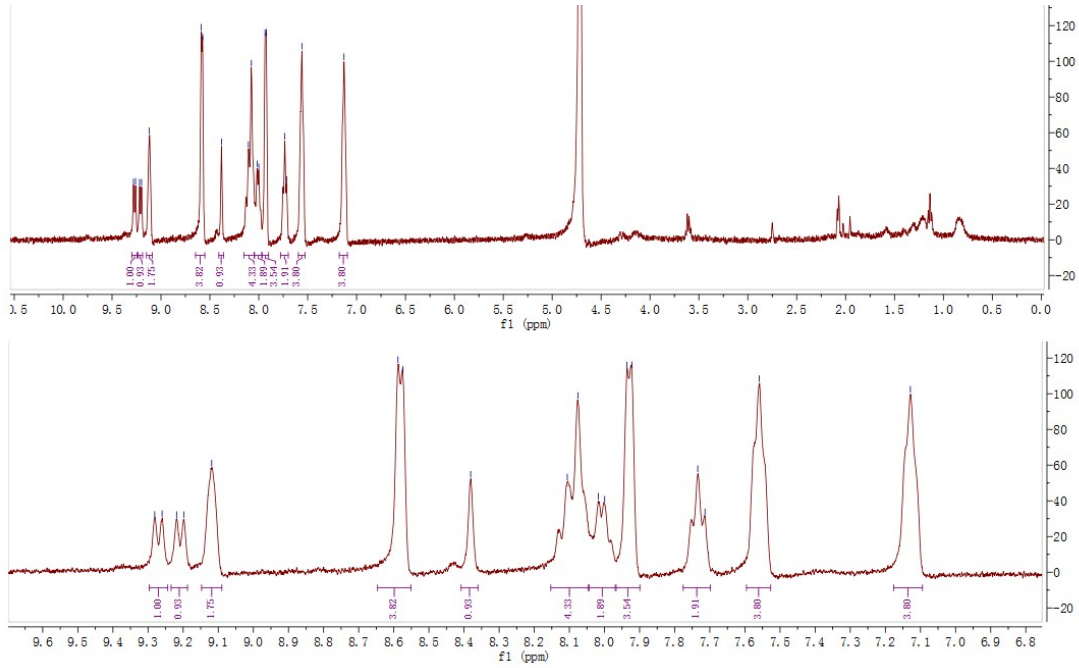

Figure S6. ^{1}H-NMR of [Ru(CF_3-dppz)($py)_4$]($Cl)_2$ (**4**) in deuterated water.

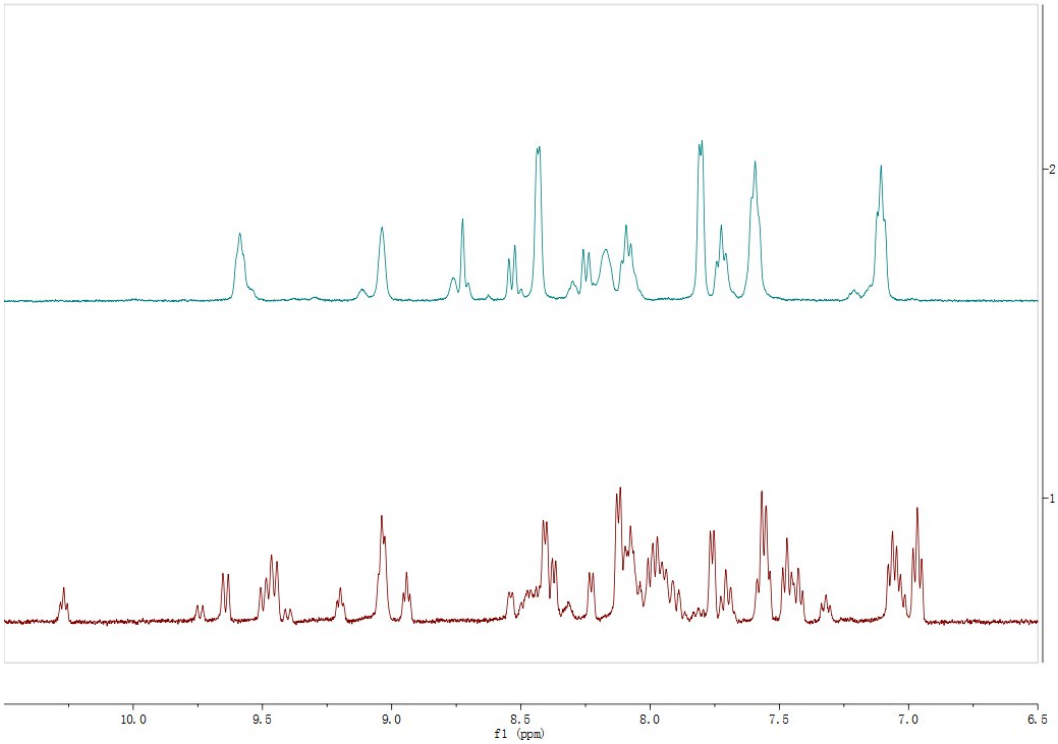

Figure S7. ^{1}H-NMR of complex **4** (top, in CD_3CN), and **4** after irradiation (bottom, 470 nm, 27 J/cm^2) in physiological saline. The irradiated sample was removed of solvent (and free pyridine in the process) and excess NaCl, and redissolved in CD_3CN.

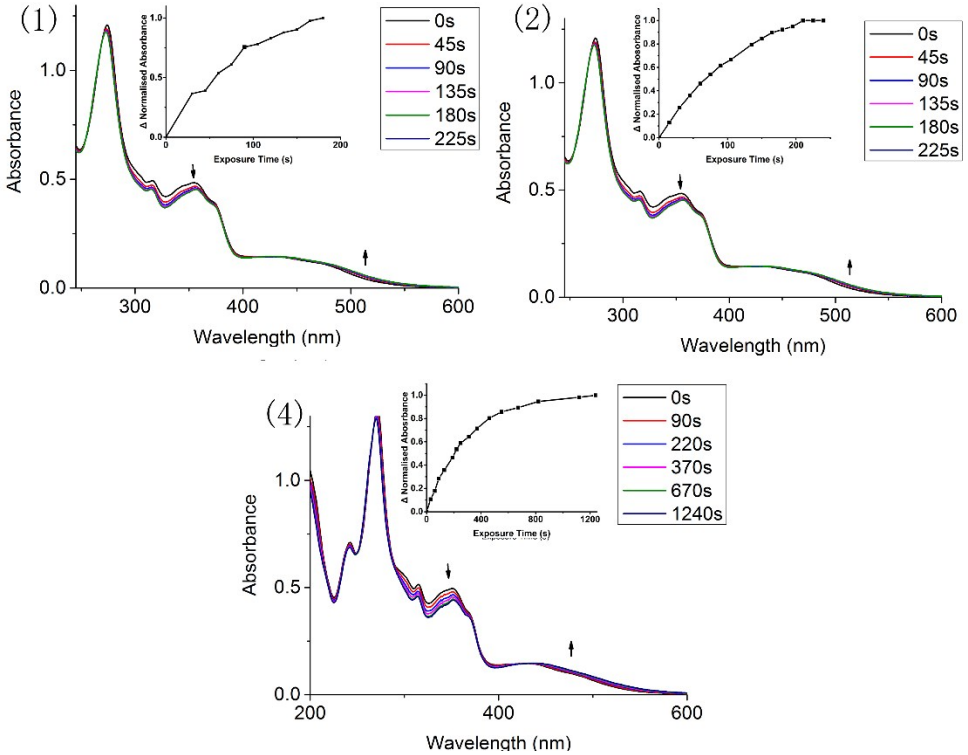

Figure S8. Absorption spectra changes of $[Ru(dppz)(py)_4](Cl)_2$ (**1**), $[Ru(F\text{-}dppz)(py)_4](Cl)_2$ (**2**) , $[Ru(CF_3\text{-}dppz)(py)_4](Cl)_2$ (**4**) (40 μM) in H_2O upon irradiation (470 nm). Inset: Δnormalized absorption changes at 355 nm, 355 nm, 351 nm for complexes **1, 2, 4**, respectively.

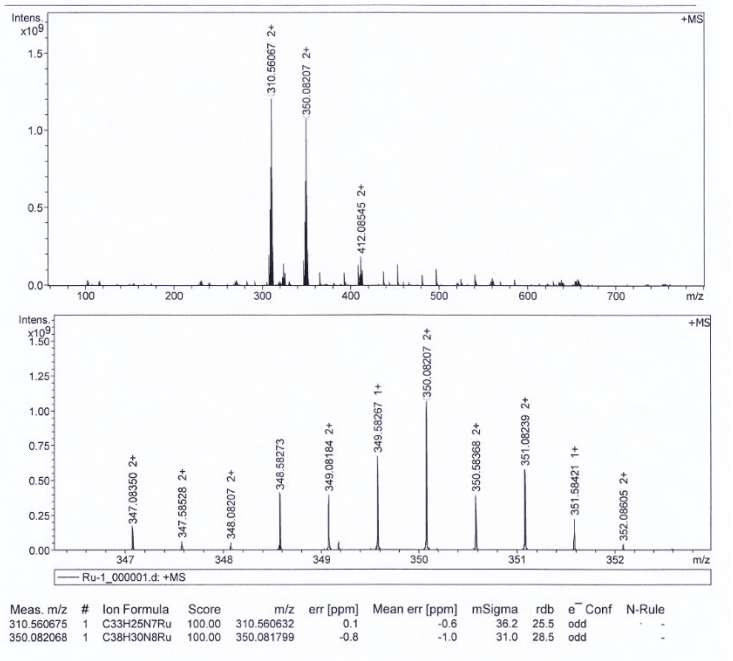

Meas. m/z	#	Ion Formula	Score	m/z	err [ppm]	Mean err [ppm]	mSigma	rdb	e⁻ Conf	N-Rule
310.560675	1	C33H25N7Ru	100.00	310.560632	0.1	-0.6	36.2	25.5	odd	-
350.082068	1	C38H30N8Ru	100.00	350.081799	-0.8	-1.0	31.0	28.5	odd	-

Figure S9. ESI mass spectra of $[Ru(dppz)(py)_4](Cl)_2$ (**1**).

$[Ru(dppz)(py)_4]^{2+}$ =$[C_{38}H_{30}N_8Ru]^{2+}$: calculated: 350.08180, Found: 350.08207.

$[Ru(dppz)(py)_3]^{2+}$ =$[C_{33}H_{25}N_7Ru]^{2+}$: Calculated: 310.56063, Found: 310.56067.

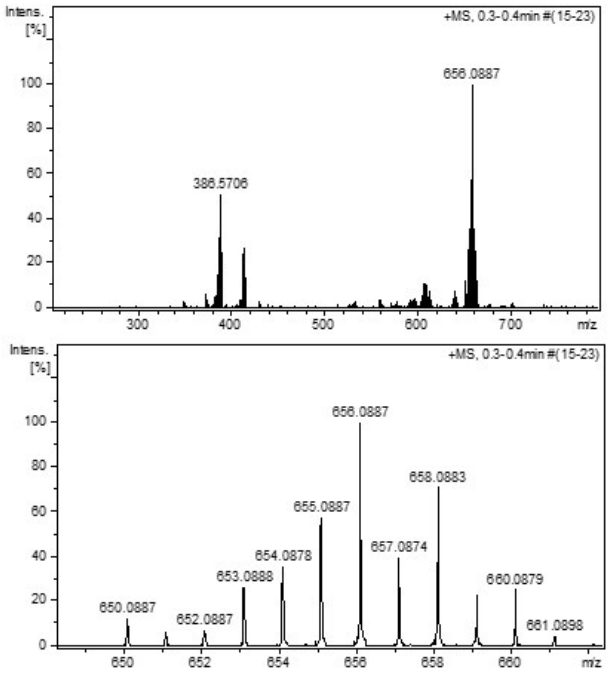

Figure S10. ESI mass spectra of $[Ru(dppz)(py)_4](Cl)_2$ (**1**) after irradiation (470 nm, 27 J/cm^2, 20 min) in physiological saline. One pyridine ligand was substituted by Cl^-.

$[Ru(dppz)(py)_3(Cl)]^+$ =$[C_{33}H_{25}N_7ClRu]^+$:calculated: 656.0898, Found: 656.0887

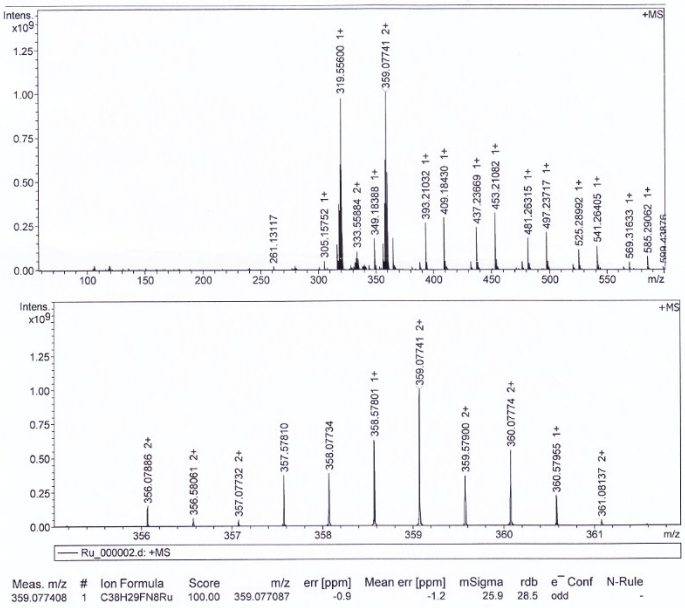

Meas. m/z	#	Ion Formula	Score	m/z	err [ppm]	Mean err [ppm]	mSigma	rdb	e⁻ Conf	N-Rule
359.077408	1	C38H29FN8Ru	100.00	359.077087	-0.9	-1.2	25.9	28.5	odd	-

Figure S11. ESI mass spectra of $[Ru(F\text{-}dppz)(py)_4](Cl)_2$ (**2**).

$[Ru(F\text{-}dppz)(py)_4]^{2+}$ =$[C_{38}H_{29}FN_8Ru]^{2+}$: Calculated: 359.07709,Found: 359.07741.

$[Ru(F\text{-}dppz)(py)_3]^{2+}$ =$[C_{33}H_{24}FN_7Ru]^{2+}$: Calculated: 319.55549, Found: 319.55600.

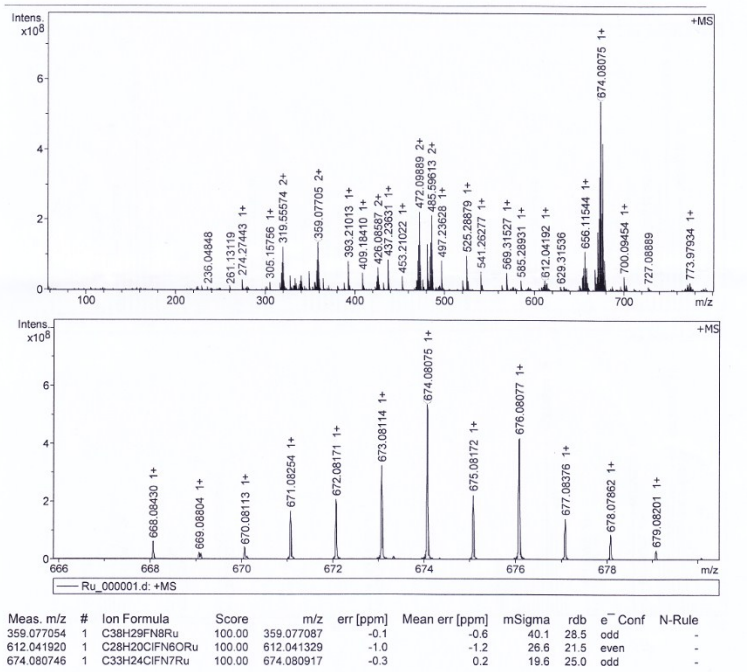

Meas. m/z	#	Ion Formula	Score	m/z	err [ppm]	Mean err [ppm]	mSigma	rdb	e⁻ Conf	N-Rule
359.077054	1	C38H29FN8Ru	100.00	359.077087	-0.1	-0.6	40.1	28.5	odd	-
612.041920	1	C28H20ClFN6ORu	100.00	612.041329	-1.0	-1.2	26.6	21.5	even	-
674.080746	1	C33H24ClFN7Ru	100.00	674.080917	-0.3	0.2	19.6	25.0	odd	-

Figure S12. ESI mass spectra of $[Ru(F\text{-}dppz)(py)_4](Cl)_2$ (**2**) after irradiation (470 nm, 27 J/cm^2, 20 min) in physiological saline. One pyridine ligand was substituted byr Cl^-.

$[Ru(F\text{-}dppz)(py)_3(Cl)]^+$ =$[C_{33}H_{24}ClFN_7Ru]^+$: Calculated: 674.08092, Found: 674.08075

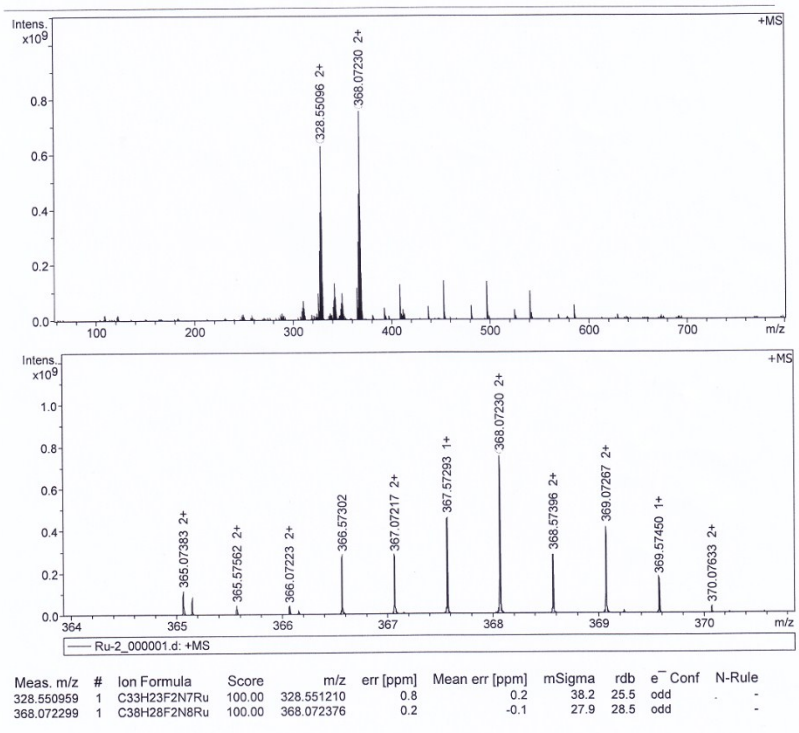

Meas. m/z	#	Ion Formula	Score	m/z	err [ppm]	Mean err [ppm]	mSigma	rdb	e⁻ Conf	N-Rule
328.550959	1	C33H23F2N7Ru	100.00	328.551210	0.8	0.2	38.2	25.5	odd	-
368.072299	1	C38H28F2N8Ru	100.00	368.072376	0.2	-0.1	27.9	28.5	odd	-

Figure S13. ESI mass spectra of $[Ru(F_2\text{-dppz})(py)_4](Cl)_2$ (**3**).

$[Ru(F_2\text{-dppz})(py)_4]^{2+}$ =$[C_{38}H_{28}F_2N_8Ru]^{2+}$: Calculated: 368.07238, Found: 368.07230.

$[Ru(F_2\text{-dppz})(py)_3]^{2+}$ =$([C_{33}H_{23}F_2N_7Ru]^{2+}$: Calculated: 328.55120, Found: 328.55096.

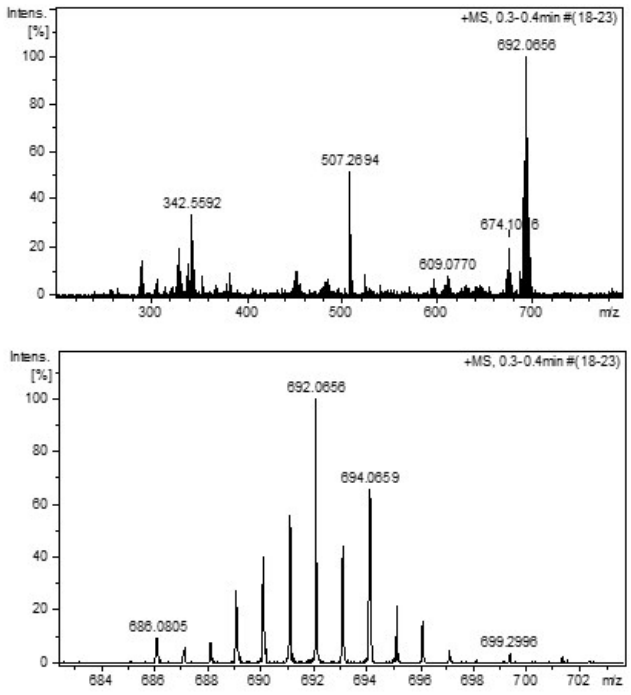

Figure S14. ESI mass spectra of $[Ru(F_2\text{-dppz})(py)_4](Cl)_2$ (**3**) after irradiation (470 nm, 27 J/cm^2, 20min) in physiological saline. One pyridine ligand was substituted by Cl^-.

$[Ru(F_2\text{-dppz})(py)_3(Cl)]^+$ =$[C_{33}H_{23}F_2N_7Ru]^+$: Calculated: 692.0709, Found: 692.0656.

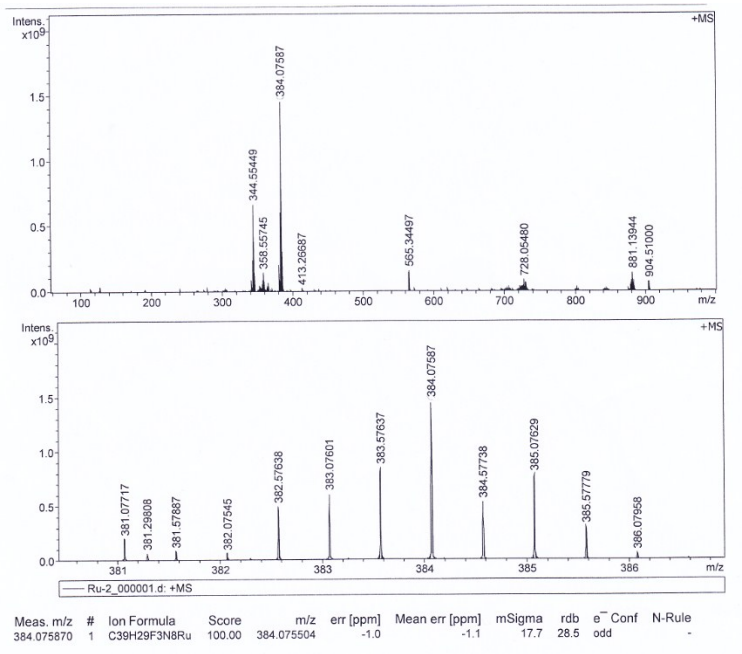

Figure S15. ESI mass spectra of $[Ru(CF_3\text{-dppz})(py)_4](Cl)_2$ (**4**).

$[Ru(CF_3\text{-dppz})(py)^4]^{2+}$ =$[C_{39}H_{29}F_3N_8Ru]^{2+}$: Calculated: 384.07550, Found: 384.07587.

$[Ru(CF_3\text{-dppz})(py)_3]^{2+}$=$[C_{34}H_{24}F_3N_7Ru]^{2+}$: Calculated: 344.55389,Found: 344.55449.

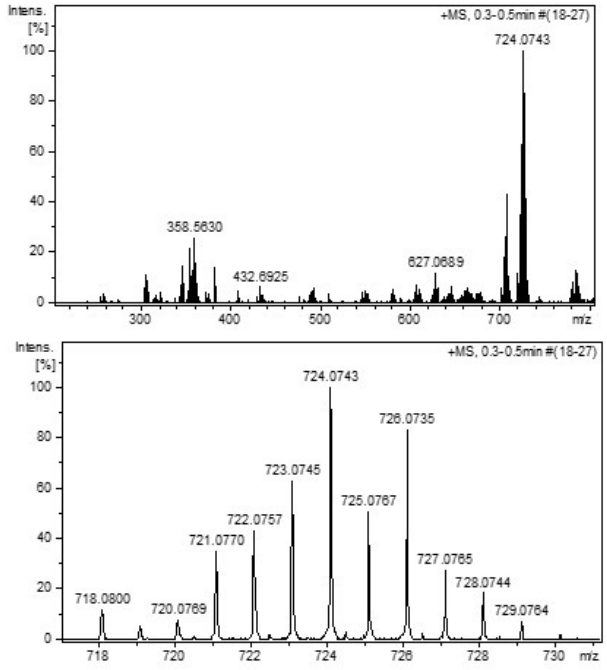

Figure S16. ESI mass spectra of $[Ru(CF_3\text{-dppz})(py)_4](Cl)_2$ (**4**) after irradiation (470 nm, 27 J/cm^2, 20min) in physiological saline. One pyridine ligand was substituted by Cl^-.

$[Ru(CF_3\text{-dppz})(py)_3(Cl)]^+$=$[C_{34}H_{24}ClF_3N_7Ru]^+$: Calculated: 724.0777, Found: 724.0743

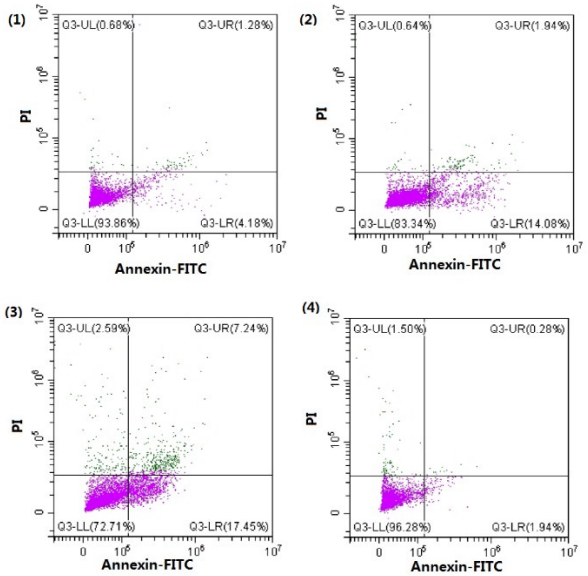

Figure S17. Percentage of apoptotic SKOV-3 cells analysed by flow cytometry. (1-3) SKOV-3 cells incubated with 2.5, 5, 10 µM $[Ru(dppz)(py)_4](Cl)_2$ (**1**) for 4 h, then irradiated for 20 min (470 nm, 27 J/cm^2) and cultured for 10 h in the dark; (4) SKOV-3 cells incubated with10 µM $[Ru(dppz)(py)_4](Cl)_2$ for 14 h and 20 min in the dark.

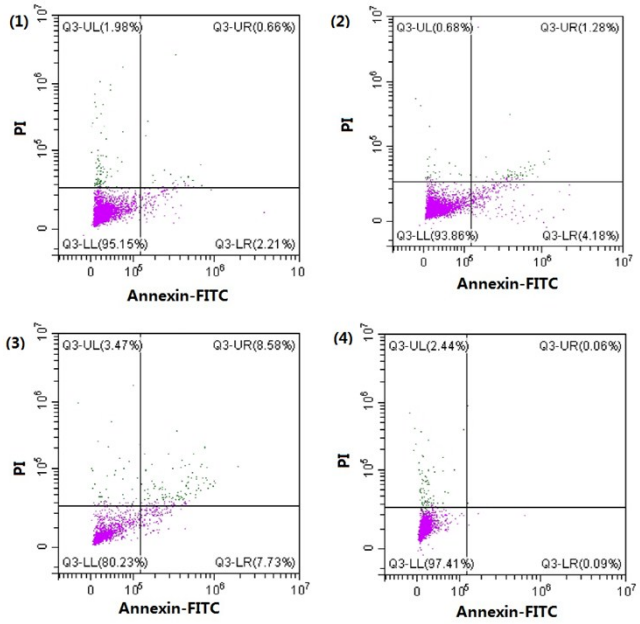

Figure S18. Percentage of apoptotic SKOV-3 cells analysed by flow cytometry. (1-3) SKOV-3 cells incubated with 2.5, 5, 10 µM $[Ru(F\text{-}dppz)(py)_4](Cl)_2$ (**2**) for 4 h, then irradiated for 20 min (470 nm, 27 J/cm^2) and cultured for 10 h in the dark; (4) SKOV-3 cells incubated with10 µM $[Ru(F\text{-}dppz)(py)_4](Cl)_2$ for 14 h and 20 min in the dark.

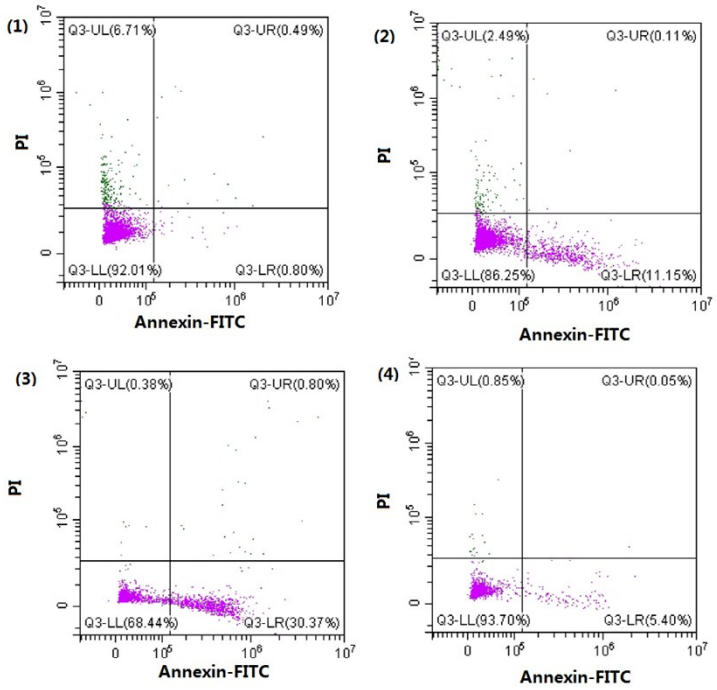

Figure S19. Percentage of apoptotic SKOV-3 cells analysed by flow cytometry. (1-3) SKOV-3 cells incubated with 2.5, 5, 10 µM $[Ru(CF_3\text{-dppz})(py)_4](Cl)_2$ (**4**) for 4 h, then irradiated for 20 min (470 nm, 27 J/cm^2) and cultured for 10 h in the dark; (4) SKOV-3 cells incubated with10 µM $[Ru(CF_3\text{-dppz})(py)_4](Cl)_2$ for 14 h and 20 min in the dark.

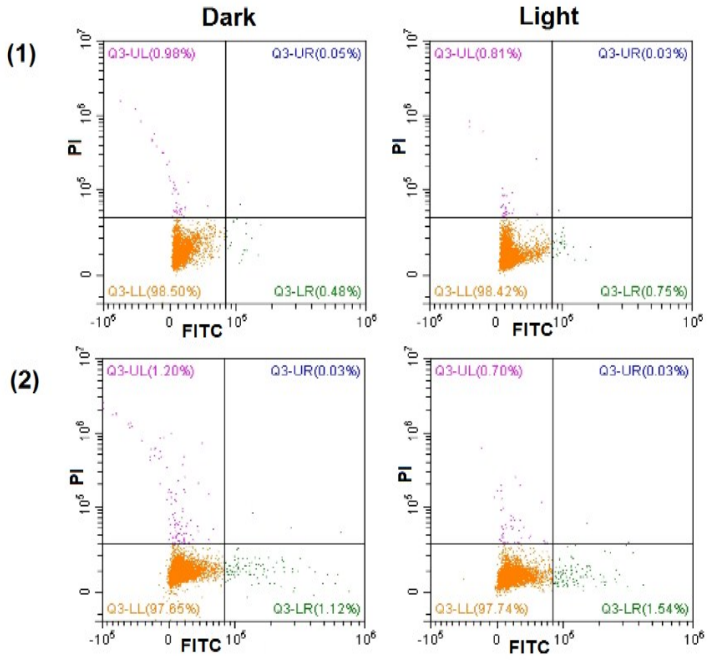

Figure S20. Percentage of apoptotic non-treated (1) HeLa and (2) SKOV-3 cells analysed by flow cytometry. Dark: cells incubated for 10 h and 20 min in the dark; Light: HeLa or SKOV-3 cells were irradiated (470 nm, 27 J/cm^2, 20 min) and cultured for 10 h in the dark.

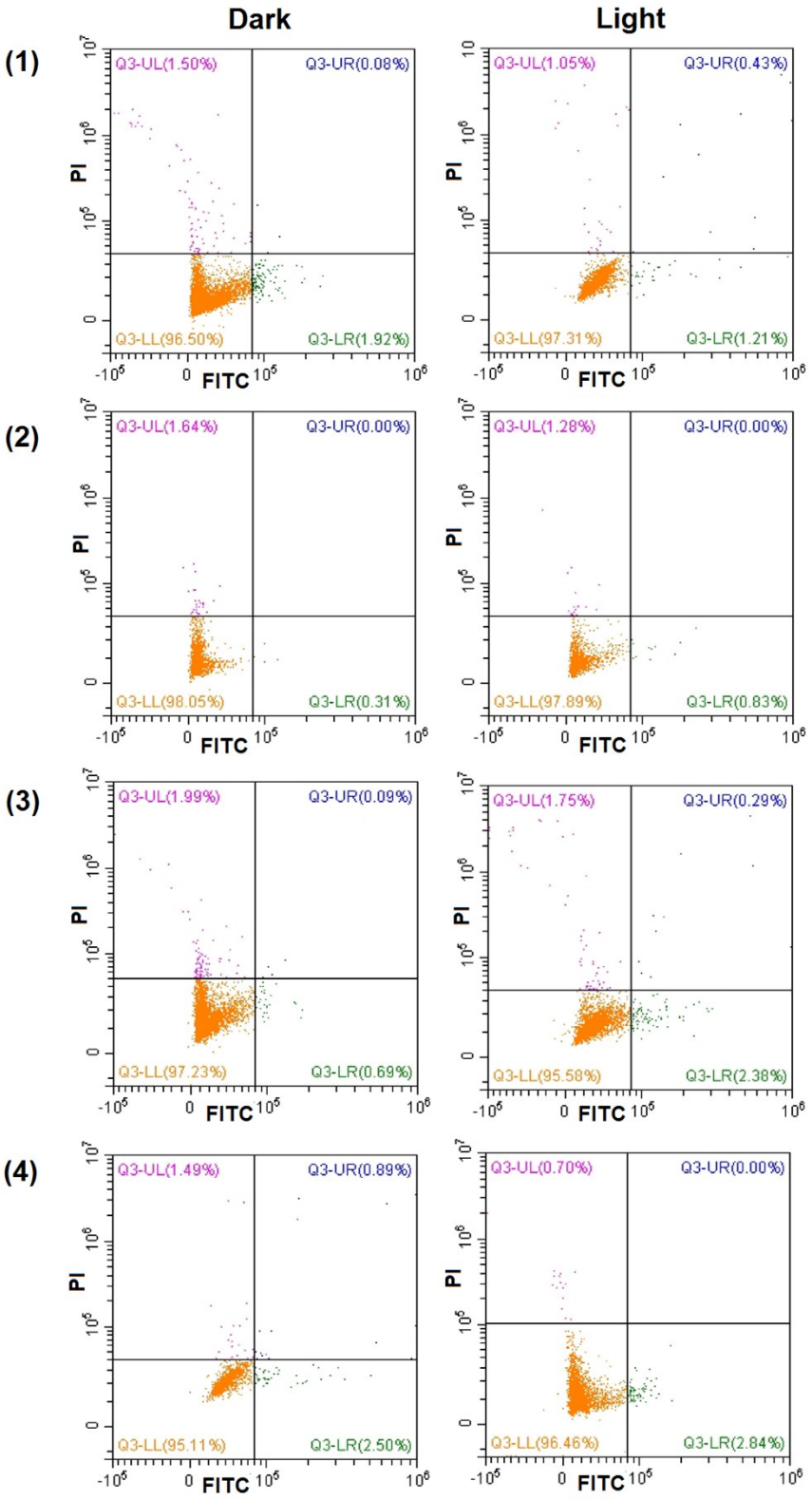

Figure S21. Percentage of apoptotic HeLa cells treated with complexes 1-4 (1 μM) upon irradiation or in the dark, then analysed by flow cytometry. Light group: HeLa cells incubated with 1 μM compounds for 4 h, then irradiated for 20 min (470 nm, 27 J/cm^2) and cultured for 10 h in the dark; dark group: HeLa cells incubated with 1 μM compounds for 14 h and 20 min in the dark.

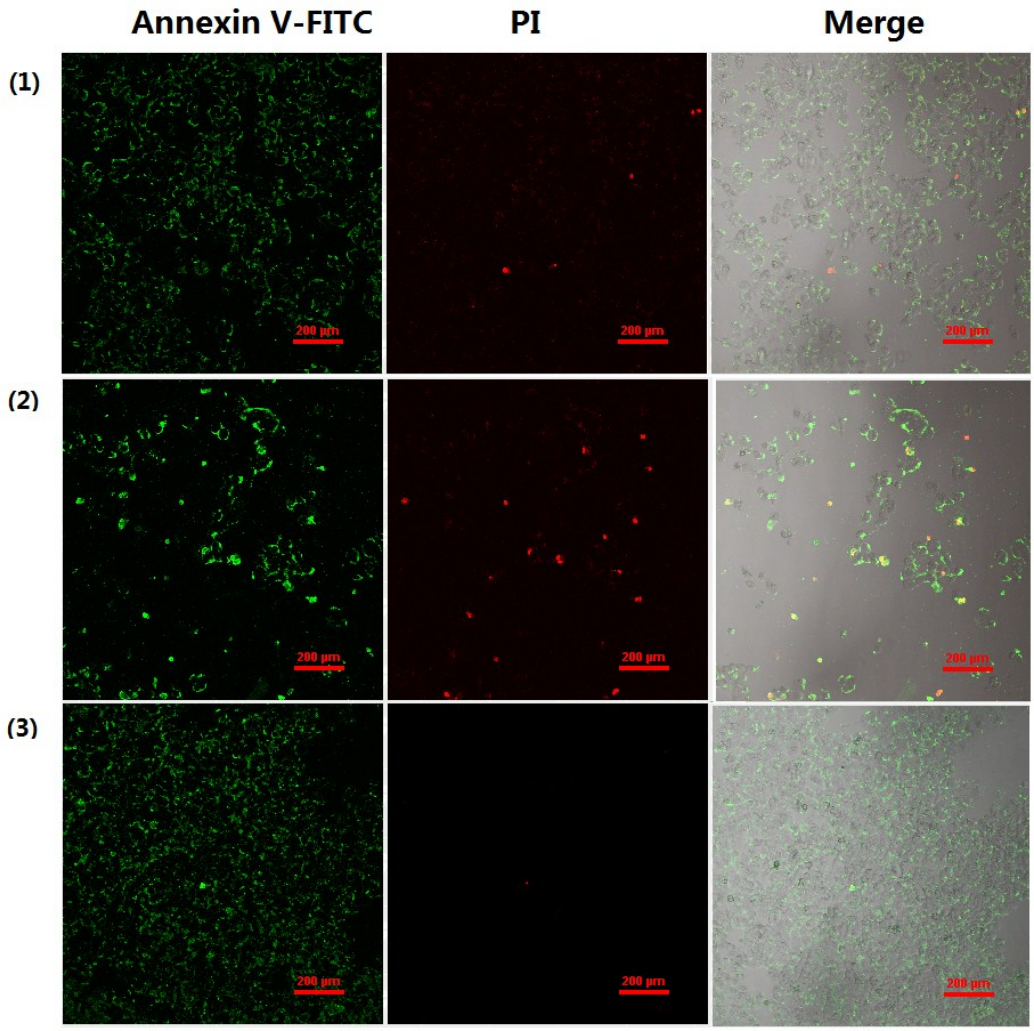

Figure S22. Annexin-FITC/PI staining of SKOV-3 cells to determine the death pathway of cells. 10 μM (1) $[Ru(dppz)(py)_4](Cl)_2$, (2) $[Ru(F\text{-}dppz)(py)_4](Cl)_2$, (3) $[Ru(CF_3\text{-}dppz)(py)_4](Cl)_2$ were incubated with cells in glass bottom dish for 4 h before irradiation with 470 nm blue light for 20min (27 J/cm^2), and the cells were cultured for another 6 h before being stained by a Annexin-FITC/PI toolkit purchased from Biodee biotechnology Co. Ltd. Green for Annexin-FITC stained cells and red for PI stained cells.

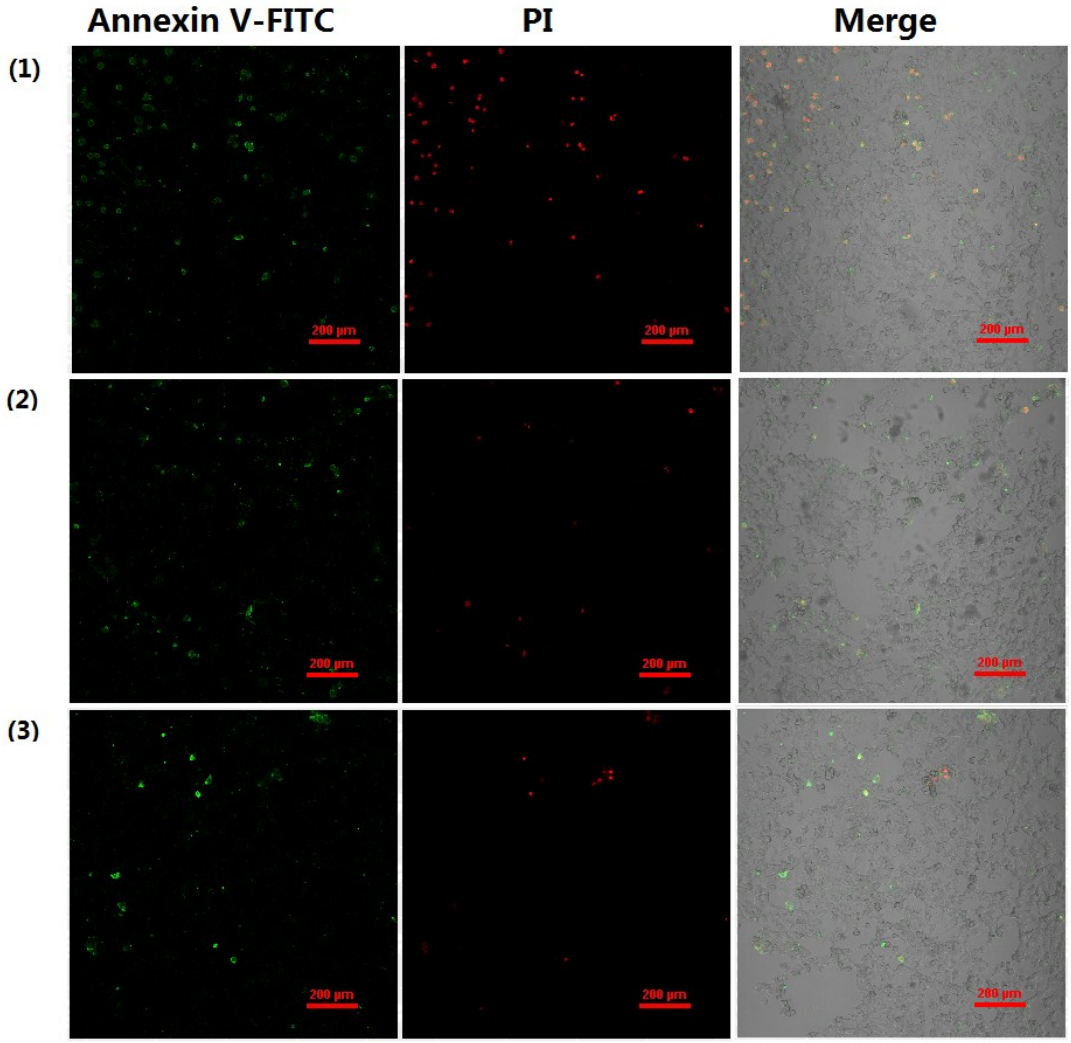

Figure S23. Annexin-FITC/PI staining of SKOV-3 cells to determine the death pathway of cells. Dark parallel experiment. 10 μM (1) $[Ru(dppz)(py)_4](Cl)_2$, (2) $[Ru(F\text{-}dppz)(py)_4](Cl)_2$, (3) $[Ru(CF_3\text{-}dppz)(py)_4](Cl)_2$ were incubated with cells in glass bottom dish for 10.33 h (4 h +20 min + 6 h) before being stained by a Annexin-FITC/PI toolkit. Green for Annexin-FITC stained cells and red for PI stained cells.

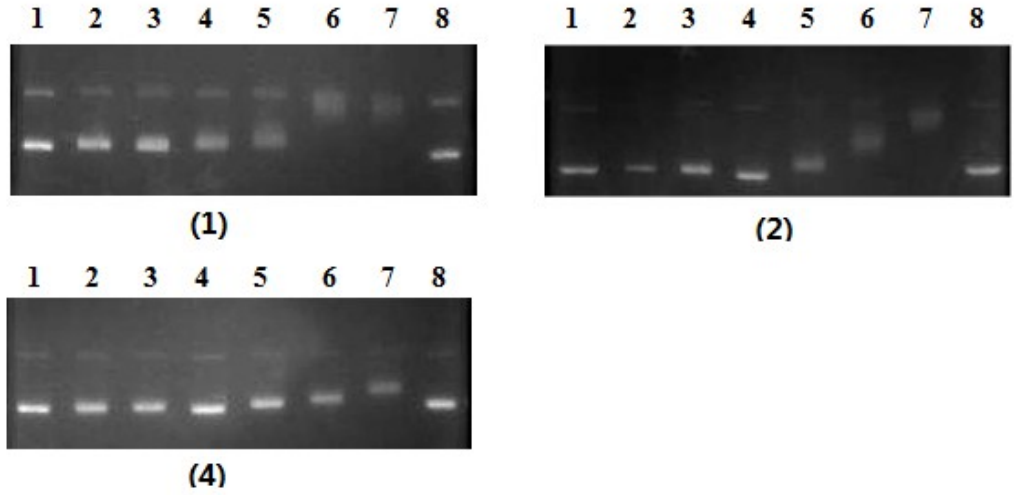

Figure S24. Agarose gel electrophoresis pattern of pBR322 DNA in the presence of varied concentrations (0, 40, 80, 20, 40, 60, 80 and 0 μM from lane 1 to 8) of complexes **1**, **2** and **4**. Lane 1-3 : dark control; lane 4-8: upon irradiation for 20 min (470 nm, 27 J/cm^2).

Table S1. IC_{50} values (μM) of complexes **1-4** when culture medium was changed before irradiation.

	HeLa		**SKOV-3**	
	light [a]	dark[b]	light [a]	dark[b]
1	57.4±1.5	>200	53.4±1.5	>200
2 [c]	>200	>200	>200	>200
3 [c]	>200	>200	>200	>200
4 [c]	>200	>200	>200	>200

[a] after 4 h of incubation with gradient concentrations of complexes **1-4,** the culture medium was changed and cells were exposed to blue light for 20 min (470 nm, 27 J/cm^2), and then was incubated for 20 h. [b] Cells incubated with gradient concentrations of complexes **1-4** for 24.33 h (4 h+20 min+20 h). [c] none of the complexes **2-4** induced noticeable reduction in cell viability in either light or dark conditions up to 200 μM when medium was changed before irradiation.